LAWRENCE
LIVERMORE
NATIONAL
LABORATORY

UCRL-CONF-222375

Modeling Hemispheric Detonation Experiments in 2-Dimensions

W. M. Howard, L. E. Fried, P. A. Vitello, R. L. Druce, D. Phillips, R. Lee, S. Mudge, F. Roeske

June 23, 2006

13th International Detonation Symposium
Norflok, VA, United States
July 23, 2006 through July 28, 2006

Modeling Hemispheric Detonation Experiments in 2 Dimensions*

W. M. Howard, L,. E. Fried, P. A. Vitello, R. L. Druce, D. Phillips, R. Lee , S. Mudge and F. Roeske.
University of California
Lawrence Livermore National Laboratory
Livermore, CA 94550

Introduction

Experiments have been performed with LX-17 (92.5% TATB and 7.5% Kel-F 800 binder) to study scaling of detonation waves using a dimensional scaling in a hemispherical divergent geometry. We model these experiments using an arbitrary Lagrange-Eulerian (ALE3D)[1] hydrodynamics code, with reactive flow models based on the thermo-chemical code, Cheetah[2]. The thermo-chemical code Cheetah provides a pressure-dependent kinetic rate law, along with an equation of state based on exponential-6 fluid potentials[3] for individual detonation product species, calibrated to high pressures (~ few Mbars) and high temperatures (20000K). The parameters for these potentials are fit to a wide variety of experimental data, including shock, compression and sound speed data. For the un-reacted high explosive equation of state we use a modified Murnaghan form[4]. We model the detonator (including the flyer plate) and initiation system in detail. The detonator is composed of LX-16, for which we use a program burn model. Steinberg-Guinan models[5] are used for the metal components of the detonator. The booster and high explosive are LX-10 and LX-17, respectively. For both the LX-10 and LX-17, we use a pressure dependent rate law, coupled with a chemical equilibrium equation of state based on Cheetah. For LX-17, the kinetic model includes carbon clustering on the nanometer size scale.

Experimental Procedures

Tests were performed to measure the detonation breakout profile and velocity in hemispherical shaped LX-17 main charges. LX-10 was used as the booster explosive for these experiments and was scaled for these shots. Two dimensions were examined – one with an overall (including booster HE) explosive radius of 43mm and the other, smaller one, with a radius of 21.5mm – half scale (fig. 1). The LX-10 booster had a radius of 15mm and 7.5mm respectively. The detonator consisted of a slapper initiating a low-density PETN pellet, which in turn throws an aluminum flyer into the booster material. The same style detonator was used for both the 43 and 21.5mm experiments. The detonator mechanics were not scaled between the two dimensions with the notable exception that the flyer driven into the booster material, from the detonator on the 21.5mm - scale shot was reduced by constricting the barrel leading to the booster – i.e, the flyer itself was scaled while the rest of the detonator remained the same size for all the experiments. In both cases a stainless steel backing extended completely across the back of the explosives. The purpose of these tests was to examine how these two

dimensions – full and half scale in a divergent geometry - will compare with each other. Do these explosive configurations scale? Finally, measurements of bridge-wire-burst to breakout time were made.

The primary diagnostics used in these tests were the electronic streak, rotating mirror streak, and a two probe Fabry Perot velocimetry pressure measurement with the probes located at 5 degrees and 81 degrees with respect to the equatorial plane of the hemisphere (fig 2). The streak camera diagnostics (rotating and electronic) were both configured to relay the image of an imaginary line drawn from one side of the shot equator traveling up to the geometric center of the pole and back down to the exact opposite position (from start) on the equator. In figure 2, notice the use of mirrors set at exactly 45 degrees to facilitate accurate relaying of the sides of the hemisphere. Optical marks on all the streak cameras have an electrical analog recorded on a fast digitizing scope for loop closure purposes. The burst voltage and current traces are also recorded on the scope so that we can get a good measurement of the burst to breakout time (function time) of the LX-17/LX-10 combination.

Fig. 3 shows the full-scale detonation breakout for shot (a) and the half-scale detonation breakout (b) timed to the bridgewire burst. The center of each streak is a view looking down directly on the pole of the hemisphere. The two side streaks are the views from the 45-degree mirrors (one is seen in figure 2) and are used to allow much higher accuracy in capturing the detonation wave at and near the equator of the hemisphere. Time is running from the top of the page towards the bottom.

Fig. 4 shows the digitized records of the detonation wave breakout for the full-scale experiment from the electronic and rotating mirror streak cameras. Time here is with respect to bridgewire burst. Likewise, Fig. 5 shows the same information from the half-scaled shot. Figure 5 shows an approximately 10 ns offset between the electronic streak data and the rotating mirror streak data. Since they are looking at the same phenomena they should be identical. The offset is unexplained, however is probably due to an unknown error in recording the timing of some component of the shot.

Fig. 6 shows the digitized plots normalized in time by multiplying the half-scale times by a factor of two. Detonator times were removed in order to look at just the LX-10/LX-17 HE scaling. If time scaled perfectly we would expect to see the two curves overlay. Note that, while the poles of the two hemispheres scale remarkably well (+- 25 degrees), the further one looks to either side of the pole position, the more deviation is seen in terms of arrival time of the detonation wave to HE surface. The percentage time difference between the half-scale and full-scale experiment at 90 degrees away from the pole is approximately 4%. However, it should be noted that at the equator the time difference is on the order of 0.25 μs (which is 4% of the total transit time from burst). This magnitude of time difference in the breakout profile could be important in certain applications.

Fabry Perot operates on the principle of Doppler shifted light. For the experiment, a pulse of 532nm light impinges upon the surface point of the HE of interest. When the detonation wave arrives at that point, the frequency of light is changed and sent back to

the analyzer room via fiber. Fig. 7 shows the analyzed Fabry records plotted as a function of Pressure vs. time with respect to bridge burst. We note that within the error of the measurement that the pressures at corresponding angles for the full and half-scale tests are essentially the same. If indeed there is a subtle difference (on the order of 10 kbar) we would have to do more experiments with a finer temporal resolution to establish that difference. To first order the output pressure at these two angles appears to scale.

Experimental Conclusions

We have performed experiments that attempt to gather data on how far we can push scaling for IHE main charges. By using LX-10 as the booster we attempted to take the booster system out of the scaling equation since in the LX-10 we expect ideal propagation of detonation waves in both full-scale and half-scale cases. The detonator was also removed from the equation by only scaling the aluminum flyer in diameter and not thickness. The diameter in the half-scale case is sufficient to promptly initiate the LX –10, which has a critical diameter of <1mm. Thus we should be left with a fairly good example of how the IHE, LX-17, is scaling in a divergent geometry.

Results show that the experiments scale generally with time to within about 4%. Details show deviations as one moves away from the pole, which could be significant in certain applications. This effect may be due to a more pronounced effect from rarefaction in the half-scale example than the full-scale one. The pressure output at 9 and 85º with respect to the equatorial plane also appears to scale within about 4%.

Model Calculations

Based on our hydrodynamics models with reactive flow, we are able to replicate the experimental results as to shock arrival times along the surface of the hemisphere. However, we find the relative breakout times along the surface of the hemisphere depend on the details of the initiation and our kinetic models. We also model a variety of detonator configurations and discuss the effect lighting on the propagation of the detonation front.

Using our kinetic models, we are able to resolve the detonation fronts with 200 zones/cm in 2-D. From such a model we are able to resolve the 2-D flow characteristics of the detonation waves and observe interesting shock interactions between the detonation waves and the detonator configuration. These experiments and our modeling provide insights into an improved understanding of detonation flow in a divergent geometry. It also demonstrates our capability to accurately model off-center detonations in 2-D using reactive flow models with a molecular-based equation of state.

For the reactive flow models we use a pressure-dependent rate law given by

$R = 0.070\ P^2 \quad \mu s^{-1}$ for LX-17

With an equation of state for the detonation products based on a multi-species, multi-phase fluids in thermo-chemical equilibrium at high pressures and temperatures. This equation of state has been validated against shock-Hugoniot, static compression and sound speed data for molecular species at high pressures and temperatures, as well as for molecular mixtures. The reactive rate laws are calibrated to give the experimental detonation velocities for LX-10 and LX-17. In addition, the LX-17 model includes a carbon-clustering model on a nanometer scale.

We consider here a kinetic based model for the solid carbon slow time scale energy release in detonation waves in the non-ideal explosive LX-17. The CHEETAH thermo chemical code was used coupled to our ALE hydrodynamics code to determine self-consistent EOS and rate equation solutions. We ignore the distinction between carbon liquid, diamond, and graphite particulate formation for simplicity and instead treat all solid carbon in the graphite phase. The full range of graphite particles sizes are reduced to two representative values, small and large with respective heats of formation of 60 kcal/mol and 7.8 kcal/mol. The smaller particles are assumed to be in chemical equilibrium with the product gas, while larger particle production is rate controlled. Our rate model consists of two rates, a fast time scale pressure squared dependent burn rate for LX-17 to products and a slower second temperature dependent Arrhenius rate for the transformation of small graphite particles to large graphite particles. Rate parameters were determined using small-scale experiments. For prompt detonation conditions where LX-17 is nearly totally burned, the fast LX-17 burn rate is on the order of microseconds, while the slower carbon rate is on the order of tens of microseconds.

The detonator is modeled in detail, with program burn for the LX-16 detonator initiator. A Steinberg-Guinan model is use to describe the aluminum 1100. We find that the emergence of the detonation wave is very sensitive to the flyer initiation of the booster LX-10. In particular, for the half-scale detonator, to replicate the experimental wave emergence from the LX-10, we had to assume that only about one-half of the flyer plate initiated the LX-10. For this case following the initiation of the LX-10 with the calculated flyer profile, gives a detonation wave that emerges first from the side, rather than the pole (as the experiment indicates).

Figures 8 and 9 show the model configuration for the full-scale and half-scale hemisphere experiments, along with calculated pressure profiles in the LX-10 and LX-17. Figure 10 shows the small and large carbon clustering in the detonation products of the LX-17.

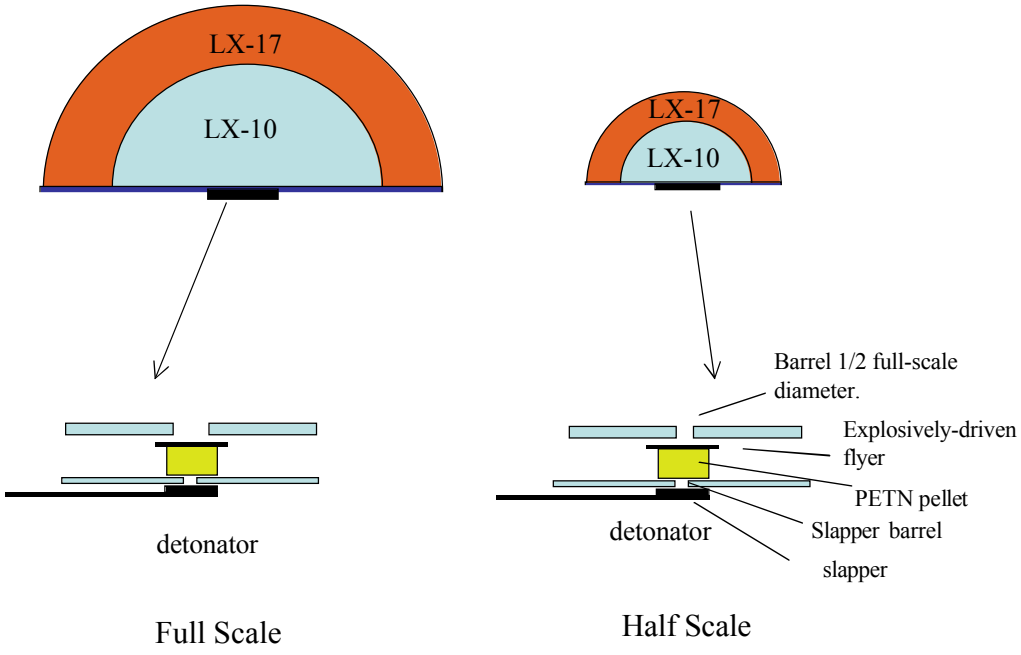

Fig 1. Cartoon of scaling of High Explosive parts. Note: Diameter of flyer barrel that drives the half- scale shot is one half that of full scale, but otherwise the detonators are the same.

Fig. 2 Mirror and probe configuration for the scaling experiments.

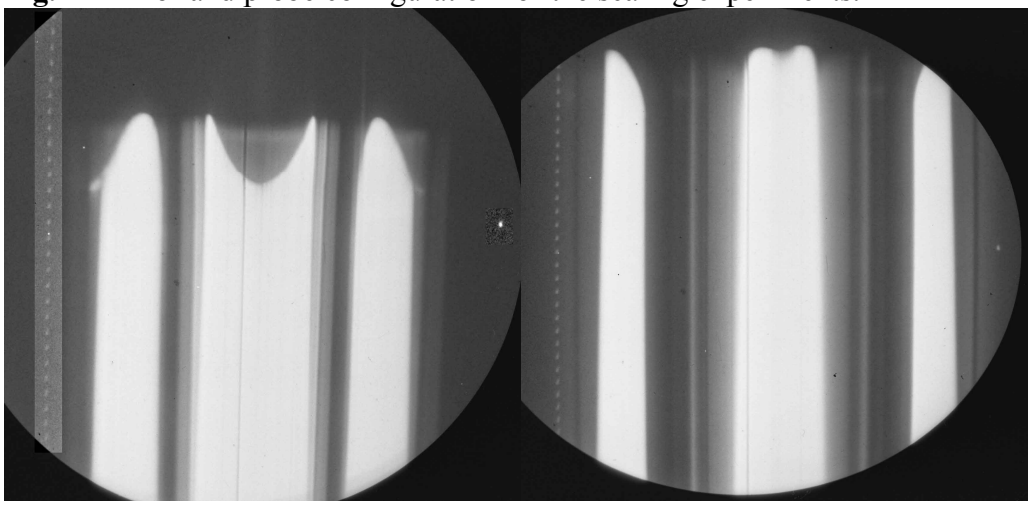

Fig.3 Raw electronic streak data for (a) full scale and (b) half-scale shots. The line of dots (comb) on the left side of each image are 25 ns apart. The timing mark, for each shot, can be seen on the right hand side of each piece of film – about half way through the sweep.

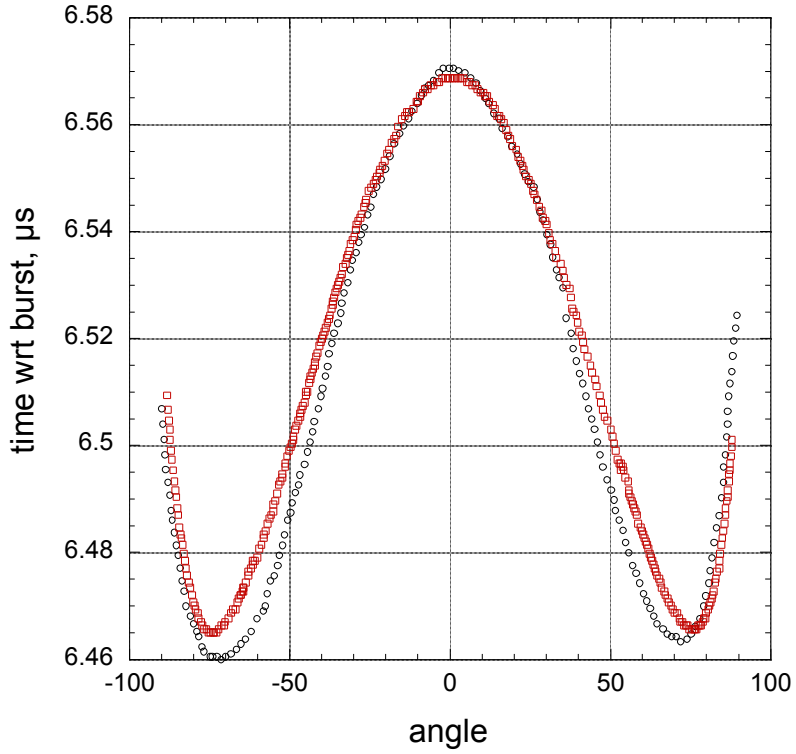

Figure 4. Full-scale detonation breakout profile .

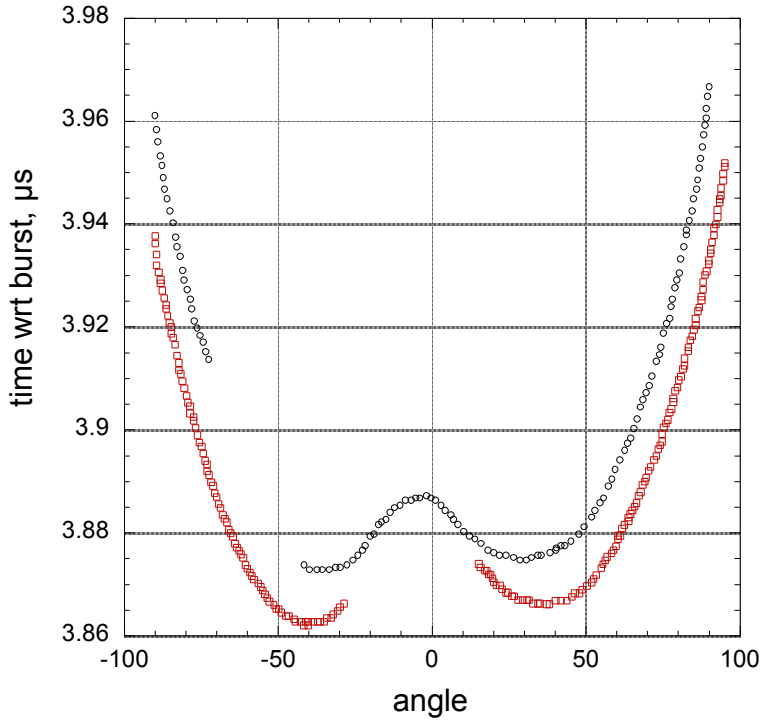

Figure 5. Half-scale detonation breakout.

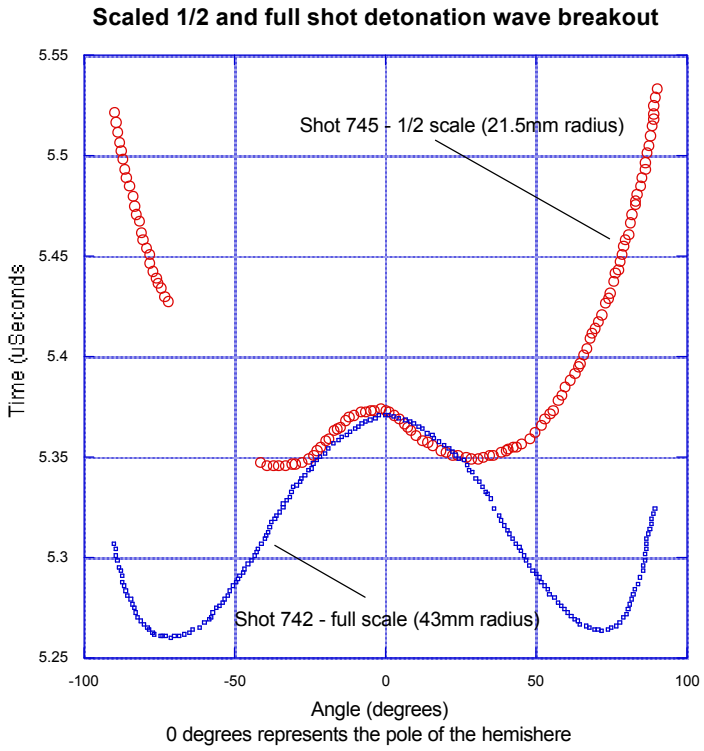

Fig. 6 Data with the half-scaled times doubled.

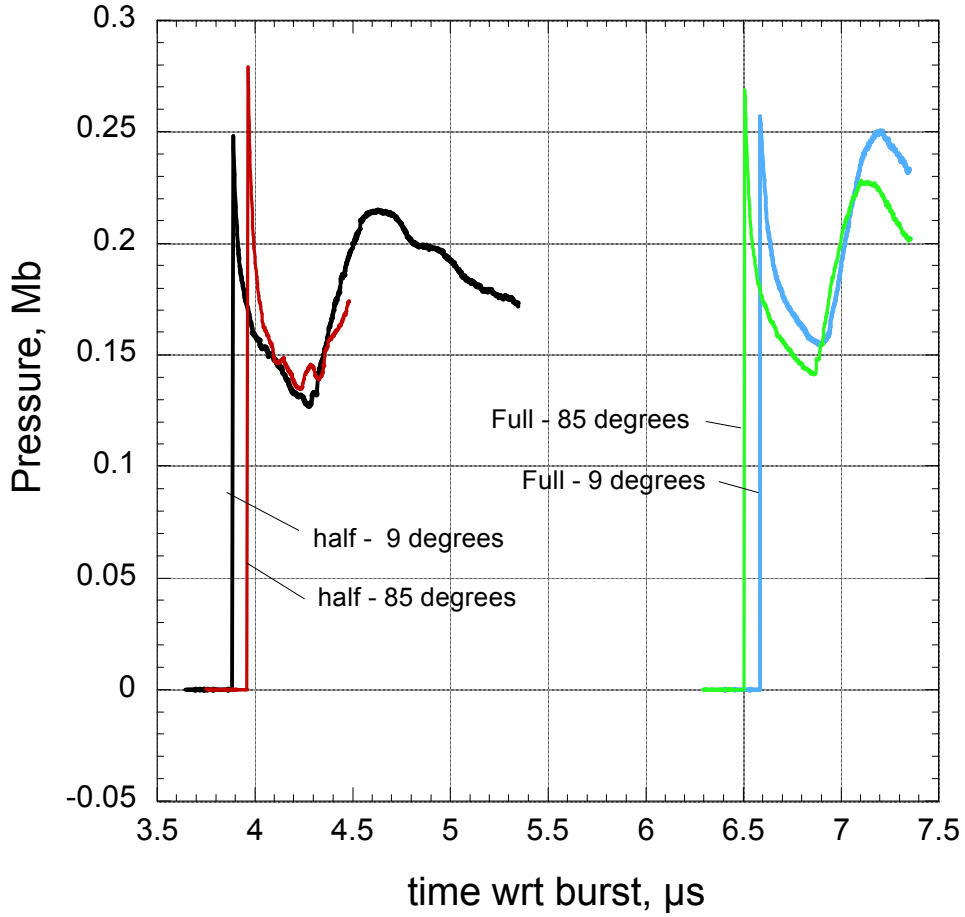

Fig. 7. Pressure comparison for full and half-scale shots at the two angle recorded.

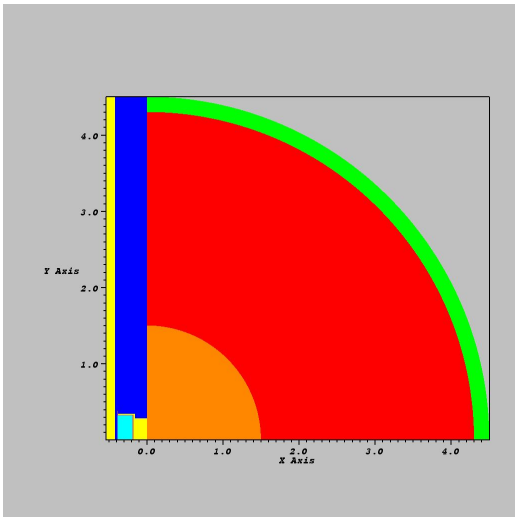

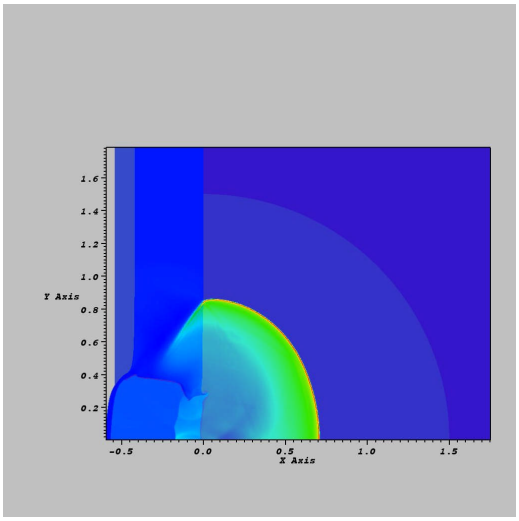

Fig. 8 The initial model configuration for the full scale hemisphere experiment. On the right is the calculated pressure wave (~ 480 kbars) in the LX-10 at a time 2.2 seconds after initiation.

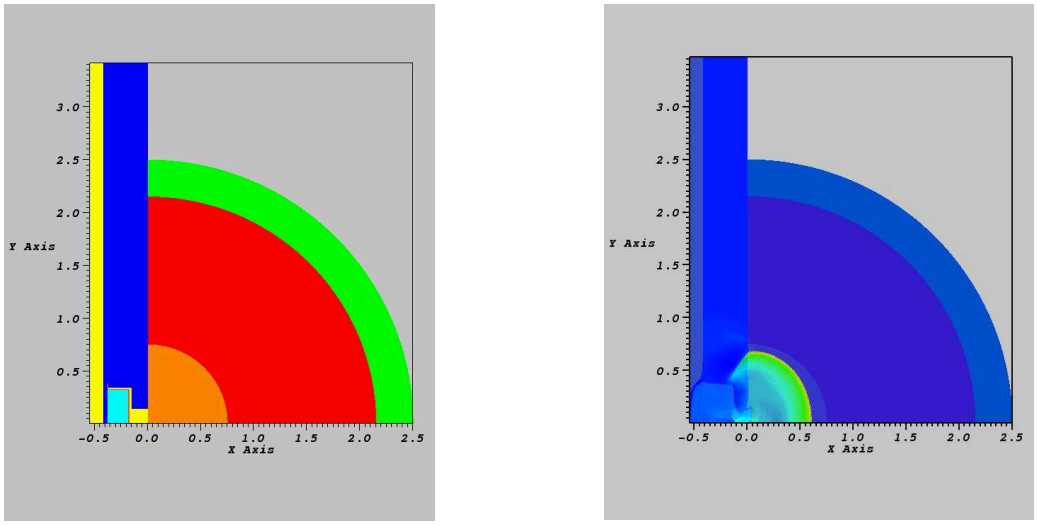

Fig. 9 The initial model configuration for the half-scale hemisphere experiment. On the left is the pressure wave (~480 kbars) in the LX-10 at a time 2.0 seconds after initiation.

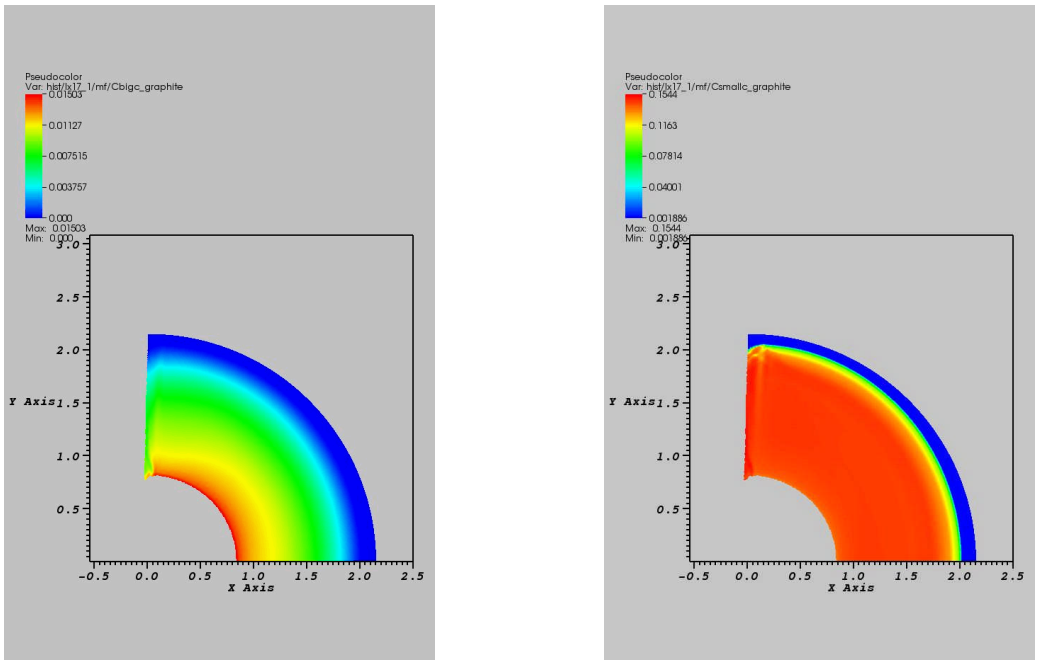

Fig. 10 The distribution of small and large carbon clusters in the detonation wave in the LX-17 for the half-scale hemisphere experiment. The small clusters compose ~ 15 percent by mass and the large carbon clusters compose ~ 1 percent by mass of the detonation products.

References

1. A. L. Nichols III, A. Anderson, R. Neely, and B. Wallin, **Proceedings Twelfth International Detonation Symposium**, Office of Naval Research, Arlington, Virginia, ONR 333-05-2, 94, 2005.
2. L. E. Fried, K. R. Glaesemann, W. M. Howard, P. C. Souers, and P. A. Vitello, Cheetah Code, version 4.0, UCRL-CODE-155944, 2005.
3. L. E. Fried and W. M. Howard, **Journal Chemical Physics**, *109*, 7338, 1998
4. L. E. Fried and W. M. Howard, **Phys. Rev. B**, *61*, 8734, 2000
5. D. J. Steinberg, S. G. Cochran and M. W. Guinan, **Journal Applied Physics**, *51*, 1498, 1980

---

*This work was performed under the auspices of the U.S. Department of Energy by University of California, Lawrence Livermore National Laboratory under Contract W-7405-Eng-48.